Journal of Electronics, Electromedical Engineering, and Medical Informatics
Multidisciplinary: Rapid Review: Open Access Journal **Vol. 5, No. 3, July 2023, pp: 125-133; eISSN: 2656-8632**

RESEARCH ARTICLE **OPEN ACCESS**

Manuscript received May 27, 2023; revised June 20, 2023; accepted June 21, 2023; date of publication July 30, 2023
Digital Object Identifier (**DOI**): https://doi.org/10.35882/jeemi.v5i3.300

How to cite: Talitha Asmaria, Andi Justike Mahatmala Zain, Arindha Reni Pramesti, Azwien Niezam Hawalie Marzuki, and Muhammad Satrio Utomo, "From Imaging Data to Cranioplasty Implant Designs, vol. 5, no. 3, pp. 125–133, July 2023.

From Imaging Data to Cranioplasty Implant Designs

Talitha Asmaria[1], Andi Justike Mahatmala Zain[2], Arindha Reni Pramesti[3], Azwien Niezam Hawalie Marzuki[3], and Muhammad Satrio Utomo[1,3,4]

[1]Research Center for Metallurgy, National Research and Innovation Agency (BRIN), South Tangerang, Indonesia
[2]Department of Physics, University of Indonesia, Depok, Indonesia
[3]Cluster of Medical Technology, Indonesian Medical Education and Research Institute (IMERI), Central Jakarta, Indonesia
[4]Department of Biomedical Engineering, University of Melbourne, Victoria, Australia

Corresponding author: Talitha Asmaria (e-mail: talitha.asmaria@brin.go.id).

ABSTRACT Cranioplasty, as a surgery to repair skull bone defects, in several patient-specific conditions, requires a personalized implant design that could match the needs. However, previous implant cranioplasty literature did not fully inform the steps to gain the patient-specific implant geometry, and not all operators could understand this sophisticated technique. The study aims to design an implant bone for cranioplasty purposes. This study will contribute as fundamental literature for implant planning since it explains an implant geometry's construction. The patient computed-scanning (CT) data were processed through the clear step-by-step image processing stages, three-dimensional (3D) printing, and its evaluation through biomechanical simulation. As the results, quantitatively, the designed cranioplasty implant could deal with the load in the actual application. Qualitatively, the prototypes have matched when applied to the host of cranium bone. In conclusion, although image processing and refinements are the most complicated process, for the following similar procedure on implant designing, the precise methodology provided in this work could significantly help the neurosurgeon and teams.

INDEX TERMS Computed Tomography Image, Image Processing, Three-Dimensional Printing, Cranioplasty Procedures, Implant Designs

I. INTRODUCTION

Cranioplasty is a surgical procedure designed to correct cranial defects. The objective of cranioplasty is not merely cosmetic; likewise, the maintenance of cranial deformities gives help to mental advantages and builds social exhibitions[1]. Over the last 15-20 years, there have been increased procedures for cranioplasty, for example, a journal mentioned between January 2012 and September 2020, a hospital performed more than 500 cranioplasties[2]. Many reviews-journal intended that any development and modification in the cranioplasty intervention would be always the hottest topic in the neurosurgery subject. The material utilized in cranioplasty until today ranges from polymers such as Polymethylmethacrylate (PMMA) and Polyetheretherketone (PEEK), bioceramic such as porous Hydroxiapaptite (HA) to the most expensive metal arrangement such as Titanium alloy[3]. The latest update of cranioplasty design also mentioned that the adjustable personalized design is necessary to improve the successful rate of cranioplasty application[4].

Similar experiments regarding building a customized cranioplasty design and prototypes have been numerously reported[4]. A journal of literature review also mentioned that the usage of three-dimensional (3D) printing has been a promising option, not only to print precisely fitted designs but also a possibility of low-cost material, of which most low-cost 3D printer materials were based on polymers[5]. However, based on a journal of evaluation between PEEK and titanium, there is still a paucity of high-level evidence about those two material applications in cranioplasty[6]. Besides the material selection, other factors, such as the timing of cranioplasty and body response in the post-operation every patient might be different, also contribute to the success of the procedures.

In Indonesia, the cranioplasty procedures have also been carried out. For the last case, a report from Dr. Soetomo General Academic Hospital utilized Polylactic Acid for 3D printing customization of cranioplasty[7]. In this case, they employed several software for image processing such as LightWave 3D and Materials Mimics before being printed

using a fused deposition modeling (FDM) printer. However, the paper does not mention in detail the employed image processing stages to achieve the model, eventually. Similarly, a review paper on 3D imaging, 3D printing, and 3D virtual planning for endodontics summarizes the process using a flowchart. The method of the 3D image processing, from the acquisition of the data, segmentation of the 3D images for the region of interest, and the computer-aided design (CAD) for refinement of the 3D mandibular bone was also not declared. Since the role of image processing techniques prior to the 3D printing application is critical in the medical field, including surgery and implant planning for cranioplasty, a step-by-step explanation of how they could be conducted would be helpful for prospective operators[8]. A provided method for the whole explanation would contribute to the repeatability and reproducibility in writing and future experiments.

This research aims to provide step-by-step image processing stages from the beginning of how the data is loaded, all refinement processes, and 3D printing for the medical tools, particularly for patient-specific needs. This study will present three significant contributions. First, it would be a novel paper that provides clear information on constructing an implant geometry from medical imaging data. Second, this paper delivers a biomechanical simulation through finite element analysis, contributing to validation. Third, to understand the hand-feel of the designed implant, 3D printing would help the match validation between the implant and the cranium bone as the host bone. The explained method would be helpful in all implant-bone designs in other body extremities.

II. MATERIAL AND METHOD

This research has four main stages: data acquisition and loading, 3D image segmentation and refinement, biomechanical simulation, and 3D printing and its physical evaluation.

A. DATA ACQUISITION AND LOADING

In this study, the employed data is a series of CT images of the brain area. The data is from the Husada Utama Hospital. Since the CT data was declared secondary data, ethical clearance is unnecessary for this experiment. In detail, the CT data consists of 194 slices, and each slice's thickness is 2 mm. The patient in this study is an Asian woman 55 years old and has a normal cranium bone. A spot in the frontal area of the skull bone would be simulated as the implant's intended area. The data has a window length of 40, a window width of 80, and dimensions of the main images of 512x512. In this study, we loaded the data using E3D Imaging software, as shown in FIGURE 1. The opening interface of E3D imaging software has plenty of imaging tools that are useful for further image processing steps.

B. IMAGE SEGMENTATION AND REFINEMENT

Based on previous medical image processing projects, image segmentation and refinement are carried out in many ways and conduct repetitions according to the obtained input images. Image segmentation aims to separate the region of interest from the whole data [9]. Image refinement seeks to improve the appearance of the segmented models until it meets the application standards [10]. In this study, we applied two ways of segmentation techniques. The first segmentation would be followed by plenty of image refinement to improve the segmented models' appearance, whereas the second segmentation only needs exporting to ready-to-print data. In the first segmentation, we employed the software of E3D Imaging. The first segmentation aims to achieve the frontal bone area and, from now on, be referred to as the host.

1) RECONSTRUCTION

The data that has been loaded into an E3D Imaging software would be reconstructed by choosing a tool of "Reconstruction" in the software. In this step, the reconstruction tool (Figure 1) built all 2D slices of CT images into 3D images of the skull bone.

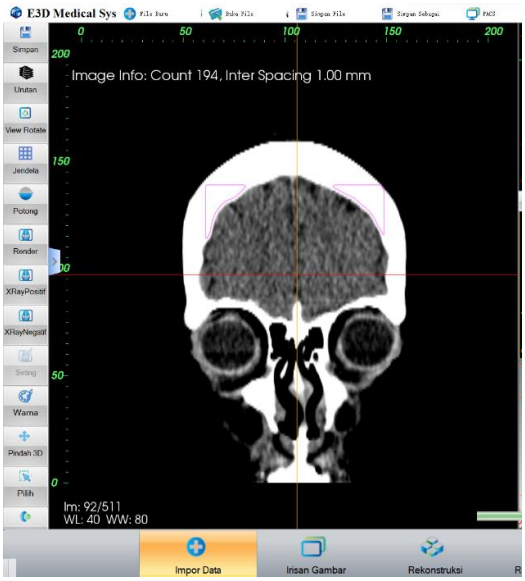

FIGURE 1. Data loading and preparing to reconstruction.

2) CUTTING

The 3D model of the skull bone was cut to achieve a selected area using a tool "cut" in the software. The head area was cut on the right, left, bottom, top, and back sides (FIGURE 2 A-D).

3) THRESHOLD SETTING

A threshold was set to the cut skull area. As early information, the threshold when the DICOM document opened was listed as 2000. The number threshold for the cut skull area can automatically be executed using the "*ambang*" feature. In this study, the cut skull area identified a threshold of 300 (FIGURE 3). This "ambang" feature would form a mask from the cut skull area.

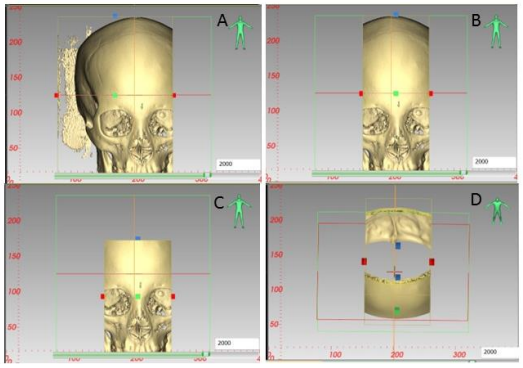

FIGURE 2. **Cutting in all dimensions. (A) right side, (B) left side, (C) upper side, (D) bottom side.**

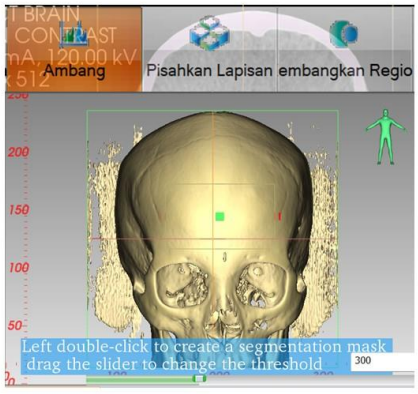

FIGURE 3. **Setting a threshold number of 300 using an "Ambang" tool.**

4) MASKED LAYERS SEPARATION

The masking selected area, particularly the frontal bone, was segmented to achieve the region of interest by using the tool of "*pisahkan lapisan*" or "separate the layers". FIGURE 4 shows the intended square area for segmentation using a masked layer.

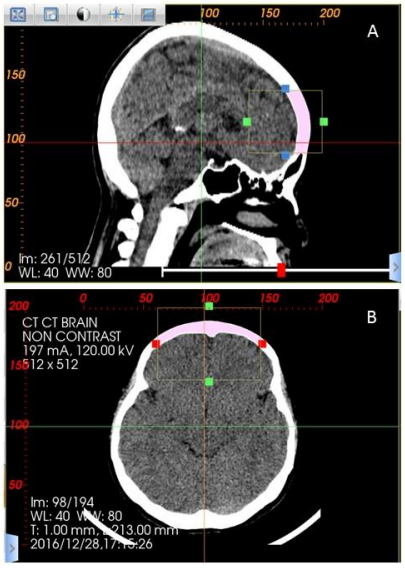

FIGURE 4. **Masking a square area of frontal bone.**

5) REGION DEVELOPMENT

The tools of "*kembangkan* region" or "develop the region" followed by the "3D calculation" option was employed to separate the selected frontal bone area from the whole subject's skull bone.

6) STL EXPORT

The final segmented model was then exported as the STL file. FIGURE 5 shows the first segmentation area for the frontal bone.

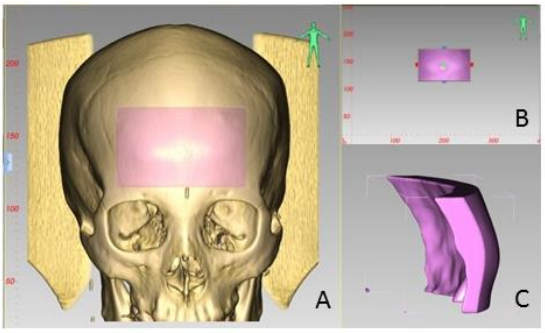

FIGURE 5. **First segmentation area of the frontal bone. (A) The area of the host implant, (B) the host implant that has been segmented from whole skull bone, (C) the surface look of the host implant.**

In the refinement process, the segmented area was then reconstructed using several tools in the software Autodesk PowerShape Ultimate (2023) under a student license. The refinement steps consist of five stages, from 7 to 11. Moreover, the second segmentation was intended to build the host of implants, representative of a small area from the whole brain, and the implant design.

7) MESH AND EDGE CONSTRUCTION

The obtained STL documents had rough and hollow surface conditions. So, it was necessary to carry out the reconstruction process to get solid STL documents with a smooth and flat surface. Once the document was imported into the software, the STL document was read as a mesh object. The first step in fixing the hollow parts was to know the location of the perforated details on the inside of the mesh, specifically by changing the view to the frontal bone object in the view menu. On the view menu, it could be selected the appearance section. The appearance menu has three view options: Shade, Wireframe, and Mesh. To see the inside of the mesh, it was then selected the Mesh option in the appearance section, followed by choosing the open and interior edges (hollow) feature. This option will make the mesh that has been selected into a transparent object composed of triangles. The mesh and edge construction are shown in FIGURE 6A.

8) FILLING HOLES

The selected surface area was filled using the continuous lasso feature. Afterward, the delete menu option on the triangles sub-menu removed the previously selected location. The holes inside the mesh can be chosen by "select the triangles then distance" and manually deleting it. The perforated meshes

must be re-filled using the fill-hole features on the "Fix panel". We could click the filling hole and curvature cap, select the gaps to fill, and then press "OK". The purpose of choosing the feature of a curvature cap was to set the filled area as high as the area according to the height of the surrounding surface. These practices were continuously done until all cavities were filled, signed by there were no yellow cavities inside of the mesh area. FIGURE 6B shows the host implant has no hole and completes the solid version.

9) SURFACE RECONSTRUCTION

The step of surface reconstruction for the mesh area was necessary to reconstruct the curvature of the mesh. The purpose of giving curved lines was to ensure that the mesh area's reshaping closely resembled the actual surface. The features of the wireframe tab, curve, and oblique curve were applied. Furthermore, the used number of curved lines to reconstruct the mesh could be determined in the section settings. The greater the number of lines used, the higher the obtained accuracy. In this case, we employed a hundred curved lines with an offset of 0. For additional notes, the higher the line number used would affect the workload of the application. In determining the axis, it could be seen through the axis options located at the bottom of the application: the x, y, and z axes. For example, the last curved line would be formed to follow the x-axis of the mesh. After practicing setting the best lines and axes in the mesh reconstruction, we could click apply. FIGURE 6C shows the task for surface reconstruction automatically by the software.

10) SURFACE RESHAPING

To build the surface formation, all formed points can be connected by using a feature of "Smart Surface" on the tab "Surface". FIGURE 6D shows the smart surface feature in Autodesk. In the settings box of the smart surface feature, it could be selected the surface type of "power surfaces" and the method of "from separate". The advanced option was utilized due to the irregularly formed surface. In this option, the setting was changed from "Automatic point and/ Guide-curve insertion" to using NURBS and for the edge matching option to be "repoints". By choosing the "Tab View" and "unblank" features, the preview feature would indicate if the shape was appropriate. After the surface has been successfully formed, the initial mesh can be compared with the resulting surface that has been developed. Next, the holes were filled and closed on both sides of the surface. Since there were already curved lines and repoints, the smart surface could be manufactured by using the surface tab, smart surface feature, and fill-in features on both sides. After successfully forming a new surface, previous curved lines could be removed by going to the home tab, panel selection, all wireframe selection, all curved lines selection, moving to the delete panel, and applying the X items.

11) FINAL SOLID FORMATION

The created surface must be made into a solid object by selecting the solid menu tab on the panel form item and then selecting the automatic trim's surface. In this study, since the right and left sides of the surface cannot form a solid, the surfaces on both sides can be deleted by pressing the right mouse once and then selecting the delete option. Next, the empty area of the solid would be repaired by using the solid doctor feature on the fixed panel on the manage solid tools menu. The solid doctor menu would display the deficiencies of the solid that had been formed. If there were still holes, they could be fixed automatically by pressing the green checkmark. If it still cannot be repaired, it could keep trying to fill in the void with the "Fill hole" with the tangential surface option, then run it by pressing the green check button.

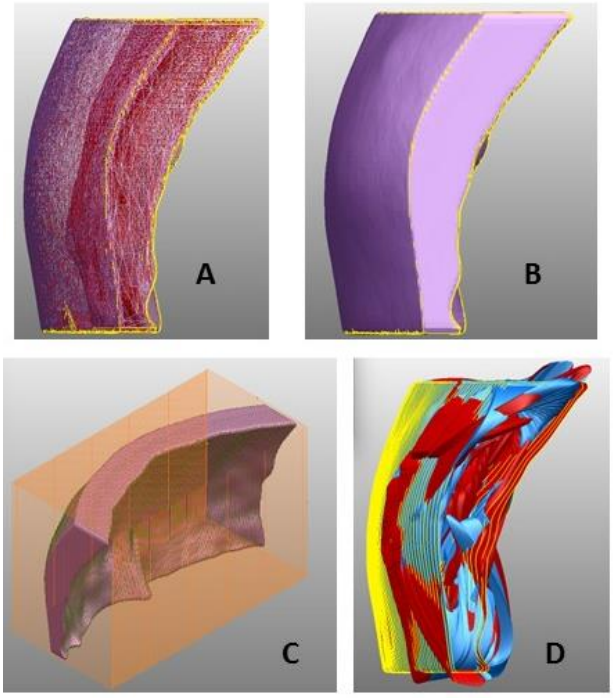

FIGURE 6. Image reconstruction stages. (A) mesh and edge construction, (B) filling hole formation, (C) surface reconstruction tool, (D) smart-surface reshaping tool.

The next step was to use the heal option. It was necessary to repair or loosen locally if the solid operation failed and the solid had no faults by pressing the green check button on the automatic option. After completing everything, it could be achieved in a solid form, as shown in FIGURE 7. Before saving to the STL format, we could select the "Triangle/Mesh" option for data exchange. In the export features, the DeltaMesh stamping option was the allowed saving option for the document type of STL. The end product from the image refinement process was a square part of skull bones. This square one represents the outer area of the implant location, called the host. In the actual cranioplasty cases, the host is possibly located in various locations with many different sizes throughout the bony area of the skull [11].

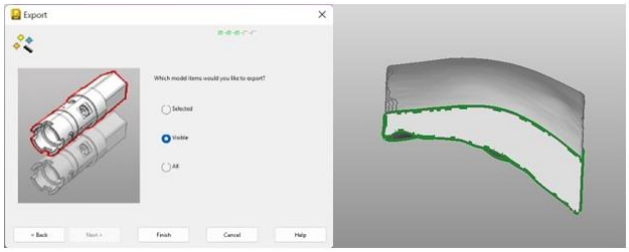

FIGURE 7. Exporting the solid formation tool using a solid doctor.

12) SECOND SEGMENTATION

The second segmentation was carried out on the Inventors software, and it aims to form two parts, namely the host and the implant. This study's final result ensures that the implant can be precise and match the host area. The first step in the second segmentation was to form a plane that would be used to sketch by selecting the sketch menu, the panel creation, and the line necessary to design the desired sketch. In this study, we used Spline (interpolation) in forming a drawing that would be used to cut the frontal bone. We could left-click once on the flat side of the frontal bone object to develop an image area. After the drawing area was formed, the design sketch could be created as desired. Next, the design was cut based on the sketch and started by opening the 3D model menu, panel modification, and selecting the split. After choosing the split feature, a dialog box of cut settings would appear, allowing it to change to the solid by pressing the green square button. Because this cut aims to be printed between the host and the implant, the selected option was keeping both sides. If the process succeeds, then two solid objects will form. It can be re-checked through the description on the model and chosen the solid bodies.

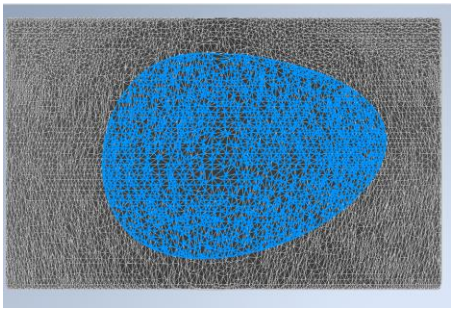

FIGURE 8. Exporting the solid formation tool using a solid doctor.

The previous design would be then stored as two separate documents between the host and the implant by adjusting the visibility of each object. Then, right-clicking on the part of the solid body enables visibility. After setting the visibility, the objects that were not shown later would not be saved when storing the STL files. For saving it separately, it could be selected in the menu file, save as, and save a copy as. Finally, a dialog box would appear, which functions to determine the type of document that is applied to save the document. This study used the STL document type. FIGURE 8 demonstrates the second image segmentation by separating the host implant with a grey area and the intended cranioplasty implant with a blue area.

C. BIOMECHANICAL SIMULATION

The biomechanical simulation in this study was done by using the software of Autodesk Inventor (Professional) 2023. The software provides materials libraries that can be determined during the FEA testing process. Determination of material can be done through material assignments and can be displayed through simulation results reports. The cranioplasty design was tested using Ti-6Al-4V material. The choice of this material is because Titanium 6Al-4V material has good biocompatibility properties and high corrosion resistance [12]. Therefore, the use of Ti-6Al-4V alloy is widely used as a material for making implants in the biomedical field. Determination of constraints and loading was carried out based on a reference for position and loading, which will be used in real conditions. The applied constraints can be in the form of fixed constraints, pin constraints, and friction constraints. For the design of this implant, using the type of fixed constraints due to the setting condition that the area around the implant will not change. While the loading is given with a load variation of 50N[13].

The process of simulating biomechanics using the finite element method can be carried out after going through the meshing and pre-analysis processes. Meshing is a process of changing the main structure into many smaller triangular elements that are a certain number to infinity. The meshing process serves to analyze the continuous system of objects. This biomechanical simulation process takes place under predetermined conditions, such as placing constraints, loading, and selecting the type of material to be tested. on the existing design. The outcomes for biomechanical simulation in this study were limited to von Misses stress (VMS). In this study case of cranioplasty, the VMS would reflect a determination if the Ti6Al4V material would yield or even fracture when given a load[14].

D. 3D PRINTING AND EVALUATION

Designs from the Autodesk Inventors software would be printed using a 3D printer of Creality Ender 5 with a material selection of poly-lactic acid (PLA) and with a nozzle size of 0.4 mm. The obtained STL would be converted into the g-code document type. Additional software of Ultimaker Cura version 5.1. enabled to print the document. Table 1 explains the setting parameters for the 3D printing process. All 3D models would be evaluated using all component tools: E3D Imaging, Autodesk Inventor, Ultimaker Cura, and the printed implant prototypes. In this study, we would compare the overall accuracy measures in the cranioplasty models, particularly the lengths of the host between the 3D models on the Autodesk Inventor and the 3D printed prototypes using a caliper. In this project, we also investigated the host length using the software E3D Imaging and Ultimaker Cura. The combination volume of the host and the implant were

also examined using the software E3D Imaging and Autodesk Inventor.

TABLE 1
3D printing settings for 3d printer of Creality Ender 5

Panel	Subpanel	Size
quality	layer height	0.15 mm
walls	wall thickness	0.8 mm
top/bottom	top/bottom thickness	0.65 mm
infill	infill density	50%
material	printing temperature	200°C
material	build plate temperature	60°C

III. RESULTS

In this result section, we will also emphasize that every step in the method section will demonstrate a similar result if redone by others.

A. DATA ACQUISITION RESULTS

In this study, we employed the E3D Medical System software as loading and image construction methods. However, since the data is in the format of DICOM, other DICOM viewer software would reveal similar details. The acquired data in this work is from an Asian woman with the age of 55 years old. This experiment utilized data from a normal patient in purpose to model a head bone structure that could later be used as a reference for cranioplasty bone implants. FIGURE 9 exhibits all details about the acquired data, however, the private information such as the name and ID patient has been kept confidential.

FIGURE 9. The acquired data was loaded in Radiant DICOM software.

B. IMAGE PROCESSING RESULTS

In the first segmentation, it was successful in obtaining the host implant section. The host implant means the outer area of the intended cranioplasty design, whereas the cranioplasty design in this study was set in the middle of the host implant place. The segmented host implant area is a specific part of the whole skull bone, particularly in the category of neurocranium bones, which generally have a structure as flat bones. The flat bones, particularly in the neurocranium, consist of the outermost layer called the pericranium, followed by the structure of compact bones and spongy bones [15]. The spongy bones, also called cancellous bones or trabecular bones, build an anatomy of a lattice-like matrix network and are not as solid as the compact bones, where there are small cavities surrounding them [16]. On the other hand, current DICOM images that contain a high amount of voxel values as well as windowing could provide a matter of grayscale on different living body tissues. This term is known as the Hounsfield unit (HU) to explain the radiodensity phenomena. It is a quantitative scale where the radiodensity of distilled water at the standard pressure and temperature (STP) is declared as 0 HU. In comparison, the radiodensity of air is -1000 HU, and the bones are between 400 and 1000 HU[17]. By this literacy, when a threshold number was applied to the segmentation process of a frontal bone, even though these bones are flat in the neurocranium, the results of the 3D frontal bone model from converting bone data in the DICOM file to STL data must have an inhomogeneous structure throughout the bones. The inhomogeneous structure resulting from the segmentation process was reconstructed in the refinement process to meet the optimal 3D stereolithography model. Lastly, the second segmentation aims to achieve the intended cranioplasty design. FIGURE 10 describes the results for both the host implant and the intended cranioplasty implant design.

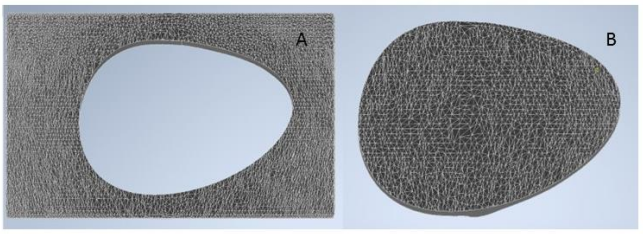

FIGURE 10. The results of the image processing stages consist of (A) the host implant area and (B) the cranioplasty implant design.

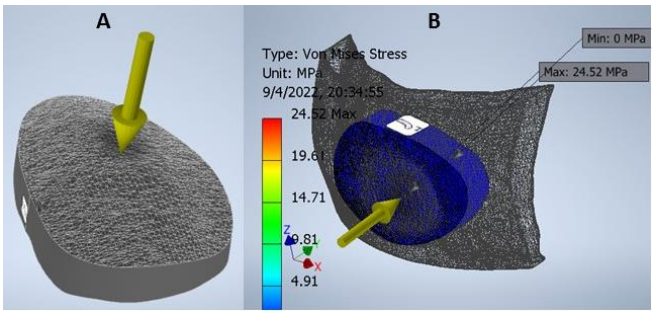

FIGURE 11. Finite element analysis. A. The placement of loading on the designed implant. B. The computer simulation to find the stress after loading the application.

C. BIOMECHANICAL SIMULATION RESULTS

After carrying out the running process using the finite element method, the results of von Misses stress (VMS) from the biomechanical simulation will be obtained. The most important aspect of this biomechanical simulation is knowing the equivalent stress or VMS. Equivalent stress occurs when a multiaxial stress state has several stress components acting simultaneously on an object structure. In this case, strain is a calculation of the force applied to an object compared to its cross-sectional area, while a strain is obtained from deformation caused by stress resulting in a change in length from the initial length. FIGURE 11A displays the constraints and loading force on the cranioplasty implant design. FIGURE 11B of the biomechanical analysis of the VMS when the implant is loaded in the y-axis direction. Based on several finite element works of literature, to determine that the built implant could be biomechanically fitted to the implanted area and have

good strength to be not easily cracked when applied, the VMS results should be less than the yield strength of the used material [12], [18]. The results of maximum VMS on the cranioplasty implant design show a lower value of 24.52 MPa than the yield strength number of Ti6Al4V of 882 MPa [19].

D. 3D PRINTING AND PHYSICAL EVALUATION RESULTS

TABLE 2 and TABLE 3 explain the physical evaluation of the parameters of length, width, and volume. Based on the length and height measurement of the host between each utilized software and the results of 3D printing, it demonstrates that during the processing and repair process, the printing process does not experience significant changes or only changes in length and height of 0.02 -0.13 mm. Meanwhile, the additional parameter in the form of the volume for the total configuration of the host and the implant design, the E3D imaging software produces a smaller volume than the volume stated on the biomechanical process using the software of Autodesk Inventor. The change in volume of 150.4 mm3 occurred because the initial sample had holes or cavities, so after processing and repair, the sample volume increased. All measured parameters verified that the results of the 3D printing application in this study are approved since all the obtained accuracy is almost 99.99%.

TABLE 2
Length and width measurement evaluation

Measurement Parameters	Length (mm)	Width (mm)
E3D Imaging	51.97	83.42
Autodesk Inventor	51.968	83.329
Ultimaker Cura	52.1	83.4
3D Prints	52.1	83.4

TABLE 3
Volume evaluation

Parameter	E3D Imaging	Autodesk Inventor
Volume (mm^3)	39748	39898.4

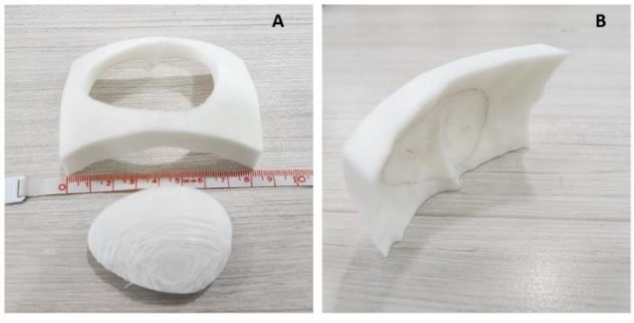

FIGURE 12. Finite element analysis. A. The placement of loading on the designed implant. B. The computer simulation to find the stress after loading the application.

For the physical evaluation, FIGURE 12A displays the 3D printing results from the host and the cranioplasty implant design. The detailed process of image refinement plays an important role in the further step of 3D printing. FIGURE 12B shows that the host and the cranioplasty implant design could fit each other, and all evaluations indicate no gap between the host and the implant. Our simulation for constructing the implant design that precisely fits the cranium bone is successful and recommended for manufacturing. FIGURE 13 represents two of the overall accuracy measures in the cranioplasty models: the lengths of the host between the 3D models on the Autodesk Inventor (FIGURE 13A) and the 3D printed prototypes using a caliper (FIGURE 13B).

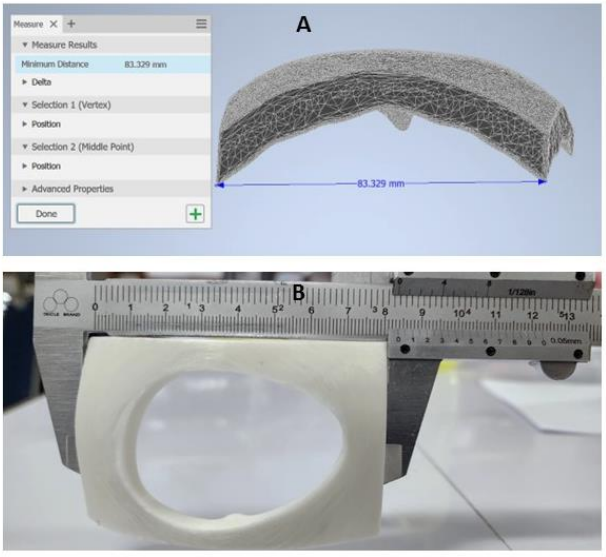

FIGURE 13. Accuracy evaluation on (A) Autodesk Inventor and (B) 3D printed prototypes using a digital caliper.

IV. DISCUSSION

This study aims to provide a renewed discourse, especially in bone implant design planning and 3D printing application. This goal has been confirmed by several lecturers and practitioners in the medical field, that this application is beneficial and helps the work of implant surgeons. The application process here has been as detailed as possible to facilitate further investigation, besides interpreting our results.

Firstly, the explanation of data acquisition and loading has proved that the medical imaging data, particularly in DICOM format, can be loaded in all DICOM viewer software. Many DICOM viewer software exist, such as Radiant DICOM, OSIRIX, 3D Slicer, Mango, etc. [20][21]. Secondly, the decision for the image processing stages depends on the region of interest of the research object. The procedures for the first segmentation in this study also considered the available features of the E3D DICOM imaging software, in which other DICOM imaging software might have different elements for image segmentation purposes. Furthermore, this study simulated a design in that the patient only needs around 5 cm diameter for the rough circle area in the neurocranium bones. The simulation shows that our design could undergo the load in the cranium area. The validation stages also indicate the cranioplasty implant design could fit into the host implant area.

Compared to other DICOM viewer software in the journals [18][19], the software in this study, E3D software, can also provide similar features, such as reading the data,

3D viewing, cropping, measuring, scaling, and multiplanar reconstruction (MPR). In the segmentation process, compared to a previous study utilizing 3D Radiant DICOM, the E3D imaging software is more helpful in the smooth cutting process [22]. Moreover, other two prior studies about cranioplasty implant designs based on patient need, they declared the host as the whole skull bones, and the intended implants were the entire defect on the skull bones patients [23], [24]. The advantages of directly segmenting the intended cranioplasty implant design are precise. There will be an adjustment for extended and elevated margins between the skull bones and the cranioplasty implant design. However, the simulation using whole skull bones could cause errors due to heavy computation. The method of separating the host and the intended implant design in this study has been successfully applied in a previous study and proved effective for any possible medicinal approaches[25].

3D printing technique has great importance in the medical world. Another recent study claimed the easy implementable 3D printing workflow for the cranioplasty implant design using a paid-commercial 3D imaging software of Materialize Mimics [26]. It revealed the chronological sequences without certain employed features. As a comparison, all stages and results in this study, which specifically target medical physicist students to have an additional curriculum or a minor subject of implant planning and formation, could convince that it is feasible to be conducted and will result in a high percentage of accuracy.

This study presents a comprehensive explanation to ensure that all stages will be reproducible for other implant design purposes. The written methods in this research have provided precise information to answer the shortcomings of previous works on the same topic, where many studies were not reproducible. However, since we employed normal patient data to have a compact implant design, this study just assumes that the area has a cranial defect. Regarding other cranioplasty implant studies that already mentioned the manufacturing process, the material selection, and the application to the patient, this study limits the research scope only to the updated design based on patient-bone morphology as well as in silico tests. For further study, the cranioplasty implant model can then be tested in real clinical settings using the DICOM data of patients with bone defects using a biocompatible material, such as Ti6Al4V [27].

IV. CONCLUSIONS

This study aims to present the complex and specific stages of 3D printing for clinical medical purposes, particularly for designing bone implants, as the leading education media and additional curriculum for medical physicist students in universities. The bone implant design in this research is limited to the patient-specific case of cranioplasty. All medical image processing methods produce 3D models of the cranium bone area as the host and the cranioplasty implant design. The design has been evaluated using a finite element analysis and demonstrates good strength with a maximum von Misses number of 24.52 MPa. The physical appearance of 3D prints between the host and the implant prototypes has been compared using several techniques. The length ranges from 51.97 to 52.1 mm, the width ranges from 83.32 to 83.42 mm, and the volume ranges from 39748 to 39898.4 mm^3. Overall, the accuracy of the 3D printing method based on patient DICOM data is almost 99.99%. Since the 3D printing results show a compact design condition and fit each other, all the available methods could be a primary reference for further bone implant design applications. For future work, the designs in this research are ready to be manufactured using biocompatible materials and implemented for the patient.

REFERENCES

[1] A. Alkhaibary, A. Alharbi, N. Alnefaie, A. Oqalaa Almubarak, A. Aloraidi, and S. Khairy, "Cranioplasty: A Comprehensive Review of the History, Materials, Surgical Aspects, and Complications," *World Neurosurg.*, vol. 139, pp. 445–452, Jul. 2020, doi: 10.1016/j.wneu.2020.04.211.

[2] M. Belzberg *et al.*, "Cranioplasty Outcomes From 500 Consecutive Neuroplastic Surgery Patients," *J. Craniofac. Surg.*, vol. 33, no. 6, pp. 1648–1654, Sep. 2022, doi: 10.1097/SCS.0000000000008546.

[3] H. Mee *et al.*, "Cranioplasty: A Multidisciplinary Approach," *Front. Surg.*, vol. 9, May 2022, doi: 10.3389/fsurg.2022.864385.

[4] J. Thimukonda Jegadeesan, M. Baldia, and B. Basu, "Next-generation personalized cranioplasty treatment," *Acta Biomater.*, vol. 154, pp. 63–82, Dec. 2022, doi: 10.1016/j.actbio.2022.10.030.

[5] W. Czyżewski *et al.*, "Low-Cost Cranioplasty—A Systematic Review of 3D Printing in Medicine," *Materials (Basel).*, vol. 15, no. 14, p. 4731, Jul. 2022, doi: 10.3390/ma15144731.

[6] J. Yang, T. Sun, Y. Yuan, X. Li, H. Yu, and J. Guan, "Evaluation of titanium cranioplasty and polyetheretherketone cranioplasty after decompressive craniectomy for traumatic brain injury," *Medicine (Baltimore).*, vol. 99, no. 30, p. e21251, Jul. 2020, doi: 10.1097/MD.0000000000021251.

[7] T. Apriawan *et al.*, "Polylactic Acid Implant for Cranioplasty with 3-dimensional Printing Customization: A Case Report," *Open Access Maced. J. Med. Sci.*, vol. 8, no. C, pp. 151–155, Nov. 2020, doi: 10.3889/oamjms.2020.5156.

[8] A. Aimar, A. Palermo, and B. Innocenti, "The Role of 3D Printing in Medical Applications: A State of the Art," *J. Healthc. Eng.*, vol. 2019, pp. 1–10, Mar. 2019, doi: 10.1155/2019/5340616.

[9] Q. Wu and K. R. Castleman, "Image Segmentation," in *Microscope Image Processing*, Elsevier, 2023, pp. 119–152.

[10] Y. Qi, A. Zhang, H. Wang, and X. Li, "An efficient FCM-based method for image refinement segmentation," *Vis. Comput.*, vol. 38, no. 7, pp. 2499–2514, Jul. 2022, doi: 10.1007/s00371-021-02126-1.

[11] I. L. Putri, T. R. Aditra, T. Apriawan, D. Kuswanto, F. R. Dhafin, and M. R. Hutagalung, "A Case Report on Lateral Proboscis: A Rare Congenital Anomaly," *Cleft Palate-Craniofacial J.*, p. 105566562110664, Dec. 2021, doi: 10.1177/10556656211066434.

[12] D. Annur *et al.*, "Material Selection Based on Finite Element Method in Customized Iliac Implant," *Mater. Sci. Forum*, vol. 1000, pp. 82–89, Jul. 2020, doi: 10.4028/www.scientific.net/MSF.1000.82.

[13] A. Ridwan-Pramana, P. Marcián, L. Borák, N. Narra, T. Forouzanfar, and J. Wolff, "Structural and mechanical implications of PMMA implant shape and interface geometry in cranioplasty – A finite element study," *J. Cranio-Maxillofacial Surg.*, vol. 44, no. 1, pp. 34–44, Jan. 2016, doi: 10.1016/j.jcms.2015.10.014.

[14] Y. Guo and W. Guo, "Study and numerical analysis of Von Mises stress of a new tumor-type distal femoral prosthesis comprising a peek composite reinforced with carbon fibers: finite element analysis," *Comput. Methods Biomech. Biomed. Engin.*, vol. 25, no. 15, pp. 1663–1677, Nov. 2022, doi: 10.1080/10255842.2022.2032681.

[15] D. A. Garzón-Alvarado, A. González, and M. L. Gutiérrez, "Growth of the flat bones of the membranous neurocranium: A computational model," *Comput. Methods Programs Biomed.*, vol. 112, no. 3, pp. 655–664, Dec. 2013, doi: 10.1016/j.cmpb.2013.07.027.

[16] Z. Li, J. Wang, J. Wang, J. Wang, C. Ji, and G. Wang, "Experimental and numerical study on the mechanical properties of cortical and spongy cranial bone of 8-week-old porcines at different strain rates," *Biomech. Model. Mechanobiol.*, vol. 19, no. 5, pp. 1797–1808, Oct. 2020, doi: 10.1007/s10237-020-01309-4.

[17] A. T. Davis, A. L. Palmer, S. Pani, and A. Nisbet, "Assessment of the variation in CT scanner performance (image quality and Hounsfield units) with scan parameters, for image optimisation in radiotherapy treatment planning," *Phys. Medica*, vol. 45, pp. 59–64, Jan. 2018, doi:

10.1016/j.ejmp.2017.11.036.
[18] M. A. Sabrina *et al.*, "Simulated Analysis Ti-6Al-4V Plate and Screw as Transverse Diaphyseal Fracture Implant for Ulna Bone," *J. Biomimetics, Biomater. Biomed. Eng.*, vol. 55, pp. 35–45, Mar. 2022, doi: 10.4028/p-63a93r.
[19] M. S. Utomo, M. I. Amal, S. Supriadi, D. Malau, D. Annur, and A. W. Pramono, "Design of modular femoral implant based on anthropometry of eastern asian," *AIP Conf. Proc.*, vol. 2088, 2019, doi: 10.1063/1.5095285.
[20] D. Haak, C. E. Page, K. Kabino, and T. M. Deserno, "Evaluation of DICOM viewer software for workflow integration in clinical trials," Mar. 2015, p. 94180O, doi: 10.1117/12.2082051.
[21] D. Haak, C.-E. Page, and T. M. Deserno, "A Survey of DICOM Viewer Software to Integrate Clinical Research and Medical Imaging," *J. Digit. Imaging*, vol. 29, no. 2, pp. 206–215, Apr. 2016, doi: 10.1007/s10278-015-9833-1.
[22] P. S. Dewi, N. N. Ratini, and N. L. P. Trisnawati, "Effect of x-ray tube voltage variation to value of contrast to noise ratio (CNR) on computed tomography (CT) Scan at RSUD Bali Mandara," *Int. J. Phys. Sci. Eng.*, vol. 6, no. 2, pp. 82–90, Jun. 2022, doi: 10.53730/ijpse.v6n2.9656.
[23] S. Park, E.-K. Park, K.-W. Shim, and D.-S. Kim, "Modified Cranioplasty Technique Using 3-Dimensional Printed Implants in Preventing Temporalis Muscle Hollowing," *World Neurosurg.*, vol. 126, pp. e1160–e1168, Jun. 2019, doi: 10.1016/j.wneu.2019.02.221.
[24] R. De Santis, T. Russo, J. V. Rau, I. Papallo, M. Martorelli, and A. Gloria, "Design of 3D Additively Manufactured Hybrid Structures for Cranioplasty," *Materials (Basel).*, vol. 14, no. 1, p. 181, Jan. 2021, doi: 10.3390/ma14010181.
[25] J. Li *et al.*, "Automatic skull defect restoration and cranial implant generation for cranioplasty," *Med. Image Anal.*, vol. 73, p. 102171, Oct. 2021, doi: 10.1016/j.media.2021.102171.
[26] J. P. Pöppe, M. Spendel, C. Schwartz, P. A. Winkler, and J. Wittig, "The 'springform' technique in cranioplasty: custom made 3D-printed templates for intraoperative modelling of polymethylmethacrylate cranial implants," *Acta Neurochir. (Wien).*, vol. 164, no. 3, pp. 679–688, Mar. 2022, doi: 10.1007/s00701-021-05077-7.
[27] T. Zegers, D. Koper, B. Lethaus, P. Kessler, and M. ter Laak-Poort, "Computer-Aided-Design/Computer-Aided-Manufacturing Titanium Cranioplasty in a Child," *J. Craniofac. Surg.*, vol. 31, no. 1, pp. 237–240, 2020, doi: 10.1097/SCS.0000000000005948.

AUTHORS BIOGRAPHY

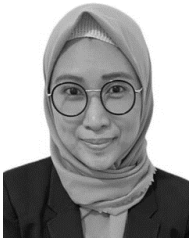

TALITHA ASMARIA received a bachelor of engineering in biomedical engineering major in 2012 from Airlangga University, Surabaya, Indonesia. She has completed her MSc degree in 2016 from biomedical engineering at the University of Bristol, United Kingdom. She is currently an early career researcher in the Research Center for Metallurgy, National Research and Innovation Agency, Indonesia, and a lecturer in the biomedical engineering study program, International University of Liasion Indonesia. Her research interest is the implant planning, which includes design analysis, image processing, material development, and 3D printing technology. She can be contacted at email: talitha.asmaria@brin.go.id

ANDI JUSTIKE MAHATMALA ZAIN was born in Kediri, East Java, Indonesia in 1999. She is currently taking a bachelor's degree in Department of Physics at the University of Indonesia. Her major interest are radio diagnostic and implants. She can be contacted at email: juztike.mz@gmail.com.

ARINDHA RENI PRAMESTI received a bachelor of engineering in biomedical engineering major in 2012 from Airlangga University, Surabaya, Indonesia. She has completed her MSc degree in 2016 from biomedical science at Gajah Mada University. She is currently an early career researcher in the medical technology cluster, Indonesian Medical Education and Research Institute (IMERI), Faculty of Medicine, University of Indonesia. Her research interest is the implant planning, which includes processing material from natural resources, scaffold for tissue engineering, 3D printing and 3D scanning technology. She can be contacted at email: arindha.reni@ui.ac.id.

AZWIEN NIEZAM HAWALIE MARZUKI was born in Jakarta, Indonesia1997. Received a bachelor Prosthetics and Orthotics in Polytechnic Health Sciene Jakarta 1 in 2019. His research interest is biomechanical and rehabilitation aspect, especially in additive manufacturing 3D printing and 3D scanning. Since 2022, he has joined with Indonesia Medical Education and Science (IMERI UI) as research assistant. He can be contacted at email: azwinnh@gmail.com.

MUHAMMAD SATRIO UTOMO received a bachelor of engineering in mechanical engineering major in 2012 from the University of Indonesia, Depok, Indonesia. He has completed her MS degree in 2015 from biomedical engineering at the Wayne State University, United State of America. He is studying as a doctoral student in the Department of Biomedical Engineering, University of Melbourne, Australia. Besides employed as an early career researcher in the Research Center for Metallurgy, National Research and Innovation Agency, Indonesia, he was also lecturer in the medical technology cluster at the Faculty of Medicine in the University of Indonesia. He can be contacted at email: muha176@brin.go.id.